RSC Advances

PAPER

View Article Online
View Journal | View Issue

Cite this: *RSC Adv.*, 2025, **15**, 20134

Diterpenoids from the aerial parts of *Isodon serra* and their anti-hepatocarcinoma potential†

Huanling Wu,‡[a] Chang Liu,‡[a] Siqin Li,[a] Chenchen Zhang,[b] Guang Yang,[b] Jiang Ma,[a] Ziying Huang,[a] Shixiong Wang,[a] Yonghao Xu,[a] Xin He *[a] and Ji Yang *[a]

Three new *ent*-kaurane diterpenoids, isodosins E–G (**1–3**), along with 20 known ones (**4–23**), were obtained from the aerial parts of *Isodon serra* (Maxim.) Hara. The structures of the new compounds were elucidated using 1D/2D NMR spectra and HREIMS data, and their absolute configurations were determined by electronic circular dichroism (ECD) calculations. The *in vitro* anti-hepatocarcinoma activities of compounds **2**, **3**, **5**, **8**, **13**, **19**, and **23** were evaluated against HepG2 and Huh7 cell lines using the CCK-8 assay. Among them, compounds **3**, **8**, and **23** exhibited high inhibitory effects on HepG2 cells, with IC_{50} values of 6.94 ± 9.10 μM, 71.66 ± 10.81 μM, and 43.26 ± 9.07 μM, respectively. In a Hepa1-6 xenograft mouse model, compound **8** significantly inhibited tumor growth at doses of 50 and 100 mg kg^{-1}, demonstrating its potent anti-hepatocarcinoma activity.

Received 18th April 2025
Accepted 6th June 2025

DOI: 10.1039/d5ra02720a

rsc.li/rsc-advances

1 Introduction

The genus *Isodon* (Lamiaceae), comprising approximately 150 species worldwide, is mainly distributed in tropical and subtropical Asia.[1] Plants of this genus are a prolific source of diverse diterpenoids with extensive biological activities, and more than 1200 diterpenoids have been isolated.[1–4] Among these diterpenoids, *ent*-kaurane diterpenoids have attracted much attention due to their promising anti-tumor activities.[5–7] For example, oridonin, a prominent *ent*-kaurane diterpenoid, has garnered widespread attention for its significant anti-tumor activity, demonstrating dose-dependent cytotoxicity against HepG2 cells with an IC_{50} value of 37.90 μM.[8,9] Numerous studies have further revealed that oridonin inhibited tumorigenesis and progression through multiple mechanisms, including induction of tumor apoptosis and autophagy, suppression of the cell cycle progression, and inhibition of angiogenesis.[8,10] In terms of molecular mechanisms, it has been demonstrated to exert its anti-tumor effects through the regulation of ROS, MAPK, PI3K/Akt, Bax/Bcl-2, and NF-κB pathways.[9,11] The findings support the potential of *ent*-kaurane diterpenoids as anticancer lead compounds and highlight the need for further research and development in this field.

Isodon serra (Maxim.) Hara, which belongs to the genus *Isodon*, is predominantly distributed in Guangdong, Fujian, and Jiangxi provinces, China.[12] Traditionally, it has been used to treat various ailments, such as hepatitis, cholecystitis, jaundice, and enteritis.[13] Previous phytochemical studies of this species have led to the isolation of abundant bioactive *ent*-kaurane diterpenes, including enmein, spirolactone, C-20 non-oxygenated, and C-20 oxygenated types.[1,14–16] These compounds have demonstrated significant pharmacological activities, including cytotoxic, antibacterial, and anti-inflammatory activities.[16,17] In our previous research, a series of *ent*-kaurane diterpenoids were isolated from the petroleum ether fraction of *I. serra*, and some of them exhibited selective cytotoxicity against HepG2 cells in the MTT assay.[18] In particular, odonicin significantly inhibited the proliferation of HepG2 cells, and this effect was achieved by inducing apoptosis.[18]

To further search for potential bioactive diterpenoids, the chemical composition of the ethyl acetate fraction from *I. serra* was investigated in the present study. As a result, three new diterpenoids (**1–3**) and 20 known ones (**4–23**) were isolated and characterized (Fig. 1). Compounds **3**, **8**, and **23** demonstrated potent inhibitory activity against HepG2 cells. Furthermore, compound **8** exhibited significant tumor growth inhibition in a Hepa1-6 xenograft mouse model.

2 Results and discussion

The aerial parts of *I. serra* were extracted three times and partitioned with petroleum ether (PE), ethyl acetate (EA), and aqueous solution (AS). The EA fraction was subjected to silica gel column chromatography, and further purified using MPLC

[a]*School of Traditional Chinese Materia Medica, Guangdong Pharmaceutical University, Guangzhou 510006, China. E-mail: hexintn@163.com; yangji@gdpu.edu.cn*

[b]*China Academy of Chinese Medical Sciences, Beijing, 100700, China*

† Electronic supplementary information (ESI) available: HR-ESI-MS, 1D/2D NMR, IR, UV, and CD data of compounds **1–3**, as well as NMR data of compounds **4–23**. See DOI: https://doi.org/10.1039/d5ra02720a

‡ These authors have contributed equally to this work.

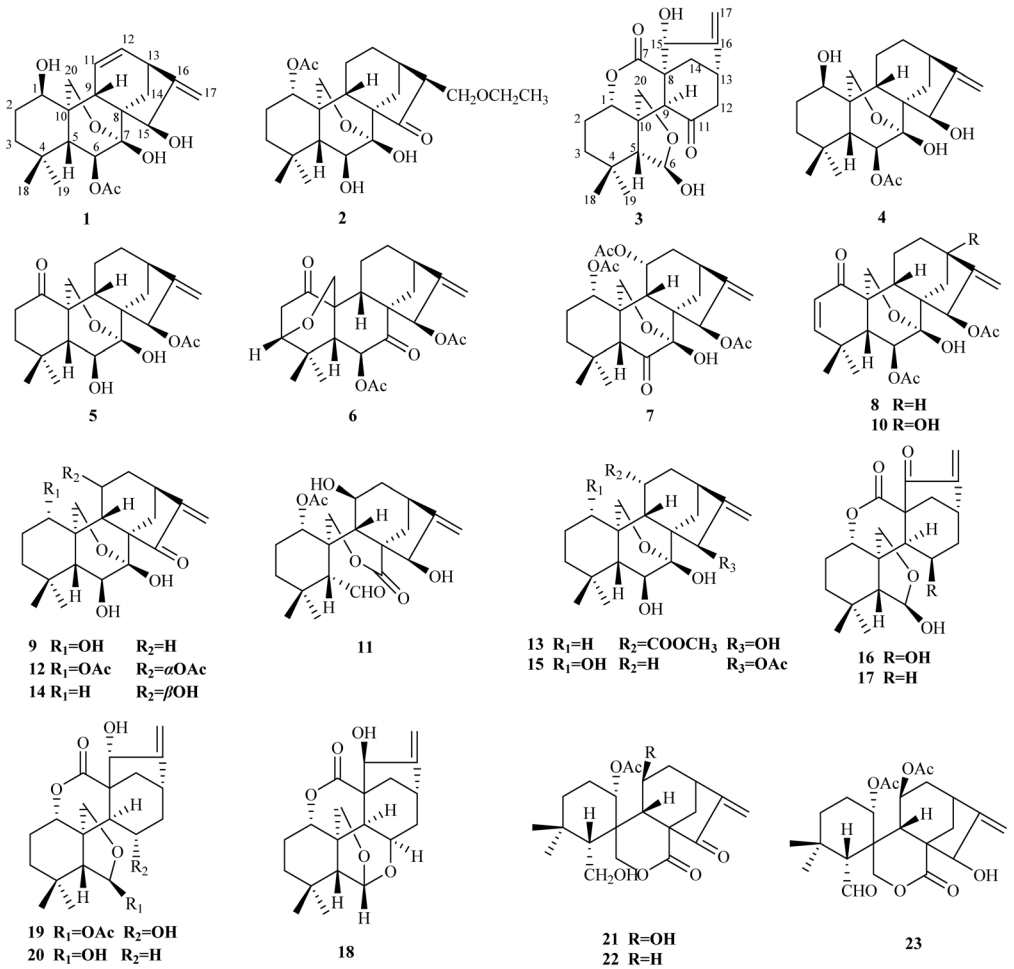

Fig. 1 Chemical structures of compounds **1–23**.

and semi-preparative HPLC. Ultimately, three new diterpenoids (**1–3**) and 20 known compounds (**4–23**) were obtained.

2.1 Structural elucidation

Compound **1**, isolated as a light yellow powder, displayed an ion peak at *m/z* 413.1950 $[M + Na]^+$ (calcd for $C_{22}H_{30}O_6Na$, 413.1935) by its HR-ESI-MS, which suggested a molecular formula of $C_{22}H_{30}O_6$ with eight degrees of unsaturation. The IR spectrum displayed the characteristic absorptions for hydroxyl (2935 cm^{-1}) and carbonyl (1738 cm^{-1}) groups (Fig. S8†). In the ^1H NMR spectrum (Table 1), three methyl singlets [δ_H 0.89 (3H, s, H-19), 1.13 (3H, s, H-18), and 2.18 (3H, s, OAc)], five oxygenated methylene or methine protons [δ_H 3.79 (1H, d, $J = 9.0$ Hz, H-20b) and 3.81 (1H, dd, $J = 9.0$, 2.5 Hz, H-20a), δ_H 3.74 (1H, m, H-1), 4.60 (1H, s, H-15), and 5.20 (1H, d, $J = 4.2$ Hz, H-6)], and four olefinic protons [δ_H 5.00 (1H, d, $J = 2.4$ Hz, H-17b), 5.05 (1H, s, H-17a), 5.76 (1H, dd, $J = 9.4$, 2.4 Hz, H-11), and 6.36 (1H, ddd, $J = 10.0$, 7.1, 2.9 Hz, H-12)] were observed. The ^{13}C NMR data revealed that **1** contained 20 carbon atoms, which were classified into three methyls, five methylenes (one olefinic and one oxygenated), eight methines (two olefinic and three oxygenated), and six non-protonated carbons (one olefinic, one ester carbonyl, and one oxygenated) by DEPT and HSQC spectra (Table 1). These data were consistent with the skeleton of a 7,20-epoxy-*ent*-kaur-16-en-1-one and were similar to those of 1β,6β,7β-trihydroxy-15β-acetoxy-7,20-epoxy-*ent*-kaur-16-ene (**4**).[19] The major difference between the two except that the two methylenes at C-11/C-12 (δ_C 26.4 and 31.7) in **4** were replaced by a double bond (δ_C 123.3 and 138.6) in **1**. This hypothesis was confirmed by the ^1H–^1H COSY correlations of H-9/H-11/H-12/H-13, as well as the HMBC correlations of H-9, H-13/C-11 (δ_C 123.3) and H-13, H-14a/C-12 (δ_C 138.6) (Fig. 2). In the NOESY spectrum, the configurations of H-1/H-11 and H-13/H-15 indicated that the hydroxyl groups at C-1 and C-15 were assigned as β-orientation. The acetoxy group at C-6 was determined to be β-oriented based on the interactions of H-6/H-20a (Fig. 3). The calculated ECD spectrum of **1** displayed Cotton Effects (CEs) analogous to the experimental ECD data, which demonstrated the absolute configuration was 1*R*,5*R*,6*S*,7*S*,8*S*,9*S*,10*S*,13*S*,15*R* (Fig. 4). Thus, the structure of **1** was elucidated and named isodosin E.

Compound **2** was obtained as a white amorphous powder. The molecular formula was determined as $C_{24}H_{36}O_7$ based on the HR-ESI-MS ion peak at *m/z* 437.2569 $[M + H]^+$ (calcd for $C_{24}H_{36}O_7H$, 437.2534), indicating seven degrees of unsaturation.

Table 1 ^{1}H NMR (600 MHz) and ^{13}C NMR (150 MHz) spectroscopic data of compounds **1–3** in $CDCl_3$ (δ in ppm, J in Hz)

	1		**2**		**3**	
Position	δ_C (type)	δ_H (mult., J in Hz)	δ_C (type)	δ_H (mult., J in Hz)	δ_C (type)	δ_H (mult., J in Hz)
1	65.5 (CH)	3.74 (m)	68.1 (CH)	5.19 (t, 4.8)	79.1 (CH)	4.62 (dd, 11.4, 5.9)
2a	26.7 (CH_2)	1.64 (m)	41.3 (CH_2)	1.46 (m)	23.5 (CH_2)	1.88 (m)
2b		1.25 (m)		1.13 (m)		1.78 (d, 12.5)
3a	33.4(CH_2)	1.78 (d, 10.3)	28.2(CH_2)	2.20 (m)	36.7 (CH_2)	1.50 (m)
3b		1.28 (m)		1.91 (dd, 16.7, 5.0)		1.54 (d, 5.3)
4	33.7 (C)		33.9 (C)		31.1 (C)	
5	51.3 (CH)	1.86 (d, 4.2)	59.8 (CH)	1.21 (d, 7.0)	54.6 (CH)	2.97 (s)
6	75.2 (CH)	5.20 (d, 4.2)	74.5 (CH)	3.78 (dd, 11.9, 7.0)	102.1 (CH)	5.34 (s)
7	97.2 (C)		94.7 (C)		173.1 (C)	
8	51.6 (C)		59.3 (C)		54.3 (C)	
9	39.8 (CH)	2.89 (d, 2.4)	52.9 (CH)	1.54 (m)	51.2 (CH)	3.79 (s)
10	41.7 (C)		36.8 (C)		47.7 (C)	
11a	123.3 (CH)	5.76 (dd, 9.4, 2.4)	18.3 (CH)	1.44 (m)	210.3 (C)	
11b				1.36 (m)		
12a	138.6 (CH)	6.36 (t, 8.2)	30.5 (CH_2)	1.34 (m)	52.5 (CH_2)	2.68 (dd, 16.0, 7.9)
12b				1.18 (m)		2.46 (d, 16.0)
13	38.6 (CH)	2.97 (dd, 7.4, 4.5)	28.6 (CH)	3.44 (m)	36.8 (CH)	3.07 (m)
14a	31.8 (CH_2)	1.95 (dd, 11.6, 4.5)	28.4 (CH_2)	2.73 (m)	36.5 (CH_2)	1.96 (dd, 12.4, 4.1)
14b		1.55 (d, 11.6)		1.95 (dd, 16.5, 9.5)		1.74 (d, 12.4)
15	74.3 (CH)	4.60 (s)	221.7 (C)		79.4 (CH)	5.24 (s)
16	155.6 (C)		56.3 (CH)	2.74 (m)	153.9 (C)	
17a	107.5 (CH_2)	5.05 (s)	66.4 (CH_2)	4.08 (d, 9.2)	111.5 (CH_2)	5.41 (s)
17b		5.00 (d, 2.4)				5.37 (s)
18	31.7 (CH_3)	1.13 (s)	33.7 (CH_3)	1.12 (s)	32.9 (CH_3)	1.08 (s)
19	21.6 (CH_3)	0.89 (s)	22.4 (CH_3)	1.10 (s)	23.7 (CH_3)	0.97 (s)
20a	66.4 (CH_2)	3.81 (dd, 9.0, 2.5)	68.8 (CH_2)	4.17 (d, 9.5)	72.1 (CH_2)	4.04 (d, 9.2)
20b		3.79 (d, 9.0)		3.70 (dd, 9.5, 3.0)		3.93 (d, 9.2)
OAc-6	170.9					
	21.4 (CH_3)	2.18 (s)				
OAc-1			169.8 (C)			
			21.9 (CH_3)	2.10 (s)		
OEt–CH_2			66.7 (CH_2)	3.49 (m)		
OEt–CH_3			15.1 (CH_3)	1.17 (t, 7.0)		

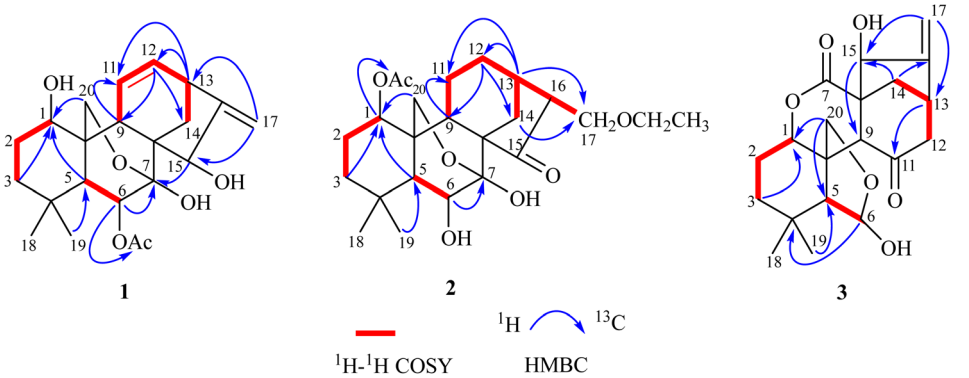

Fig. 2 ^{1}H–^{1}H COSY and key HMBC correlations of compounds **1–3**.

The IR absorption bands at 2924 and 1718 cm^{-1} suggested the existence of hydroxyl and carbonyl groups (Fig. S18†). The ^{1}H NMR spectrum of **2** (Table 1) showed signals of three methyls [δ_H 1.10 (3H, s, H-19), 1.12 (3H, s, H-18), and 2.10 (3H, s, OAc)]. The ^{13}C NMR, DEPT 135, and HSQC spectra (Table 1) revealed 24 carbon signals, including four methyls, seven methylenes, seven methines, and six non-protonated carbons (one carbonyl, one ester carbonyl, and six oxygenated). The above information indicated that the structure of **2** was similar to that of adenolin E,[20] except for two notable differences. Specifically, the methoxy group at C-17 (δ_C 68.9) in adenolin E was absent in **2** and an ethoxy group was present in **2**. Furthermore, the oxygenated methine at C-11 (δ_C 62.9) in adenolin E was replaced by a methylene group (δ_C 56.3) in **2**. These observations were also

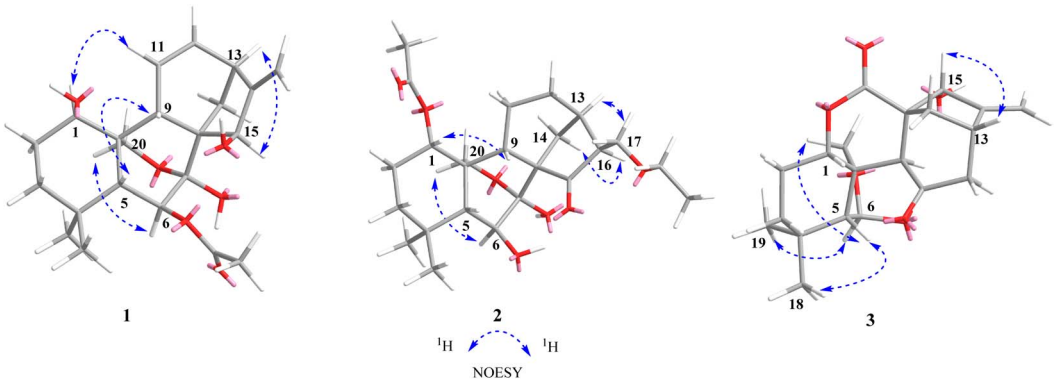

Fig. 3 Key NOESY correlations of compounds **1–3**.

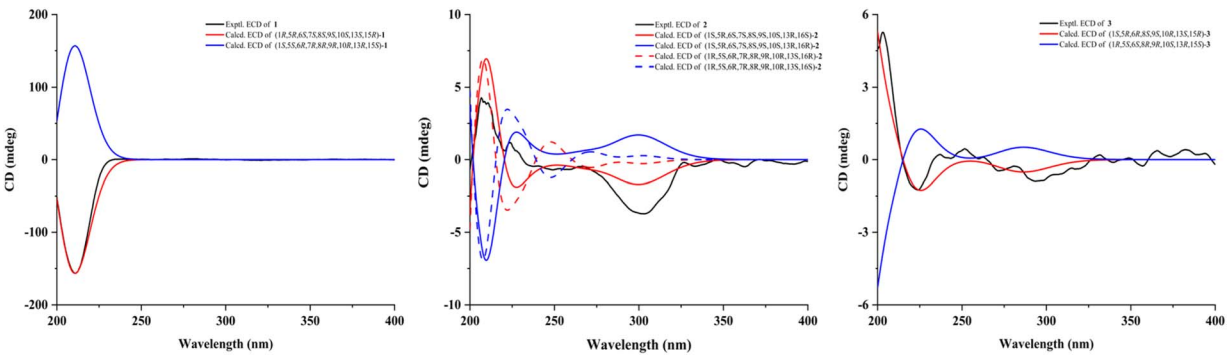

Fig. 4 Experimental and calculated ECD spectra of compounds **1–3**.

supported by ^{1}H–^{1}H COSY correlations of H-9/H-11/H-12 and the HMBC correlation of H-17 with OEt–CH_2 (δ_C 66.7) (Fig. 2). In the NOESY spectrum (Fig. 3), the correlation of H-1/H-9 indicated the acetoxy group at C-1 was α-oriented. The hydroxyl group at C-6 was β-oriented by the correlation of H-6/H-20a. The ECD spectrum of **2** was recorded in $CHCl_3$, and its absolute configuration was assigned as 1*S*,5*R*,6*S*,7*S*,8*S*,9*S*,10*S*,13*R*,16*S* by comparing the experimental data with calculated ECD curves of four possible stereoisomers (Fig. 4). Thus, the structure of **2** was elucidated and named isodosin F.

Compound **3** was obtained as a white amorphous powder, and its molecular formula was determined to be $C_{20}H_{26}O_6$ based on the HR-ESI-MS ion at *m*/*z* 385.1630 $[M + Na]^+$ (calcd for $C_{20}H_{26}O_6Na$, 385.1622), requiring eight degrees of unsaturation. Analysis of the ^{1}H NMR data of 3 (Table 1) indicated two singlet methyl groups [δ_H 0.97 (3H, s, H-19) and 1.08 (3H, s, H-18)] and two olefinic protons [δ_H 5.37 (1H, s, H-17b) and 5.41 (1H, s, H-17a)]. The ^{13}C NMR spectra of **3** showed 20 carbons classified into two methyls (δ_C 32.9, 23.7), six methylenes (δ_C 111.5, 72.1, 52.5, 36.7, 36.5, 23.5), six methines (δ_C 102.1, 79.4, 79.1, 54.6, 51.2, 36.8), and six non-protonated carbons (δ_C 210.3, 173.1, 153.9, 54.3, 47.7, 31.1), which were supported by DEPT and HSQC spectra. Analysis of its NMR data suggested many similarities to those of 6β,15α-dihydroxy-6α,20-epoxy-6,7-*seco*-*ent*-kaur-16-en-1α,7-olide (**20**),[19] with the major difference was that the methylene at C-11 (δ_C 18.6) in **20** was replaced by the ketone carbonyl group at C-11 (δ_C 210.3) in **3**. This hypothesis was confirmed by the ^{1}H–^{1}H COSY correlations of H-12/H-13/H-14 and the HMBC correlations of H-12/H-13 with C-11 (Fig. 2). The hydroxyl group at C-6 was assigned as β-oriented based on the NOESY correlations of H-1/H-5, H-5/H-18, and H-6/H-19. The α-orientation of the hydroxyl group at C-15 was deduced by the H-13/H-15 correlation (Fig. 3). The ECD curve of compound **3** showed a positive Cotton effect at 204 nm and 249 nm, which was consistent with the calculated ECD spectrum of (1*S*,5*R*,6*R*,8*S*,9*S*,10*R*,13*S*,15*R*)-**3** (Fig. 4). Thus, the structure of **3** was confirmed and named isodosin G.

The known compounds were identified as 1β,6β,7β-trihydroxy-15β-acetoxy-7,20-epoxy-*ent*-kaur-16-ene (**4**),[19] maoecrystal S (**5**),[21] neorabdosin (**6**),[22] parvifoline G (**7**),[23] odonicin (**8**),[24] effusanin A (**9**),[25] (6β,7α,15β)-6,15-bis(acetyloxy)-7,20-epoxy-7,13-dihydroxykaura-2,16-dien-1-one (**10**),[26] rabdolasional (**11**),[27] shikokianin (**12**),[28] isodoternifolin B (**13**),[29] (6β,7α,11α)-7,20-epoxy-6,7,11-trihydroxykaur-16-en-15-one (**14**),[30] maoecrystal X (**15**),[31] nodosin (**16**),[32] isodocarpin (**17**),[33] 15β-hydroxy-6,7-*seco*-6,11β:6,20-diepoxy-1α,7-olide-*ent*-kaur-16-ene (**18**),[34] 6-acetylepinodosinol (**19**),[35] 6β,15α-dihydroxy-6α,20-epoxy-6,7-*seco*-*ent*-kaur-16-en-1α,7-olide (**20**),[19] maoyecrystal E (**21**),[36] lushanrubescensin H (**22**),[37] and isorubesin C (**23**).[38] Their structures were confirmed by comparing the spectroscopic data with those previously reported, in which compounds **4–6**, **10–15**, and **19–23** were isolated from *I. serra* for the first time.

2.2 Anti-hepatocarcinoma activities *in vitro*

Hepatocellular carcinoma (HCC), as the third leading cause of cancer-related death worldwide, presents substantial therapeutic challenges due to the high rate of late diagnosis, severe side effects, and frequent drug resistance.[39–42] Diterpenoids, a structurally diverse class of natural products, have attracted considerable interest owing to their potent anti-cancer effects.[8,9]

Given the anti-cancer activity of diterpenoids from *I. serra*, the main isolated compounds **2**, **3**, **5**, **8**, **13**, **19**, and **23** were evaluated for their cytotoxic effects on HepG2 and Huh7 cell lines using the CCK-8 assay, with cisplatin as the positive control. As shown in Fig. 5 and Table 2, compounds **2**, **5**, **8**, and **23** reduced the viability of HepG2 cells in a dose-dependent manner at concentrations of 0, 12.5, 25, 50, 100, and 200 μM. Among them, compound **3** exhibited strong inhibition effects with an IC_{50} of 6.94 ± 9.10 μM, followed by compounds **23** (IC_{50} = 43.26 ± 9.07 μM) and **8** (IC_{50} = 71.66 ± 10.81 μM). By contrast, compounds **13** and **19** showed relatively weak cytotoxicity against HepG2 cells under the same conditions. In comparison, the IC_{50} value of cisplatin against HepG2 cells was 20.73 ± 5.71 μM. Notably, at a concentration of 100 μM, the inhibitory effect of compound **23** against HepG2 cells was comparable to that of cisplatin, and at 200 μM, its inhibitory effect even exceeded that of the reference drug. These results suggested that certain diterpenoids from *I. serra* exhibited promising anti-hepatocarcinoma activity.

Table 2 Effects of compounds **2**, **3**, **5**, **8**, **13**, **19**, and **23** on the proliferation of HepG2 and Huh7 cells

	IC_{50}[a] (μM)	
Compound	HepG2	Huh7
2	105.00 ± 6.49	>200
3	6.94 ± 9.10	23.34 ± 17.83
5	95.22 ± 18.86	>200
8	71.66 ± 10.81	>200
13	>200	>200
19	>200	>200
23	43.26 ± 9.07	109.60 ± 12.18
Cisplatin[b]	20.73 ± 5.71	96.15 ± 9.29

[a] IC_{50} values were means ± SD (n = 3). [b] Positive control.

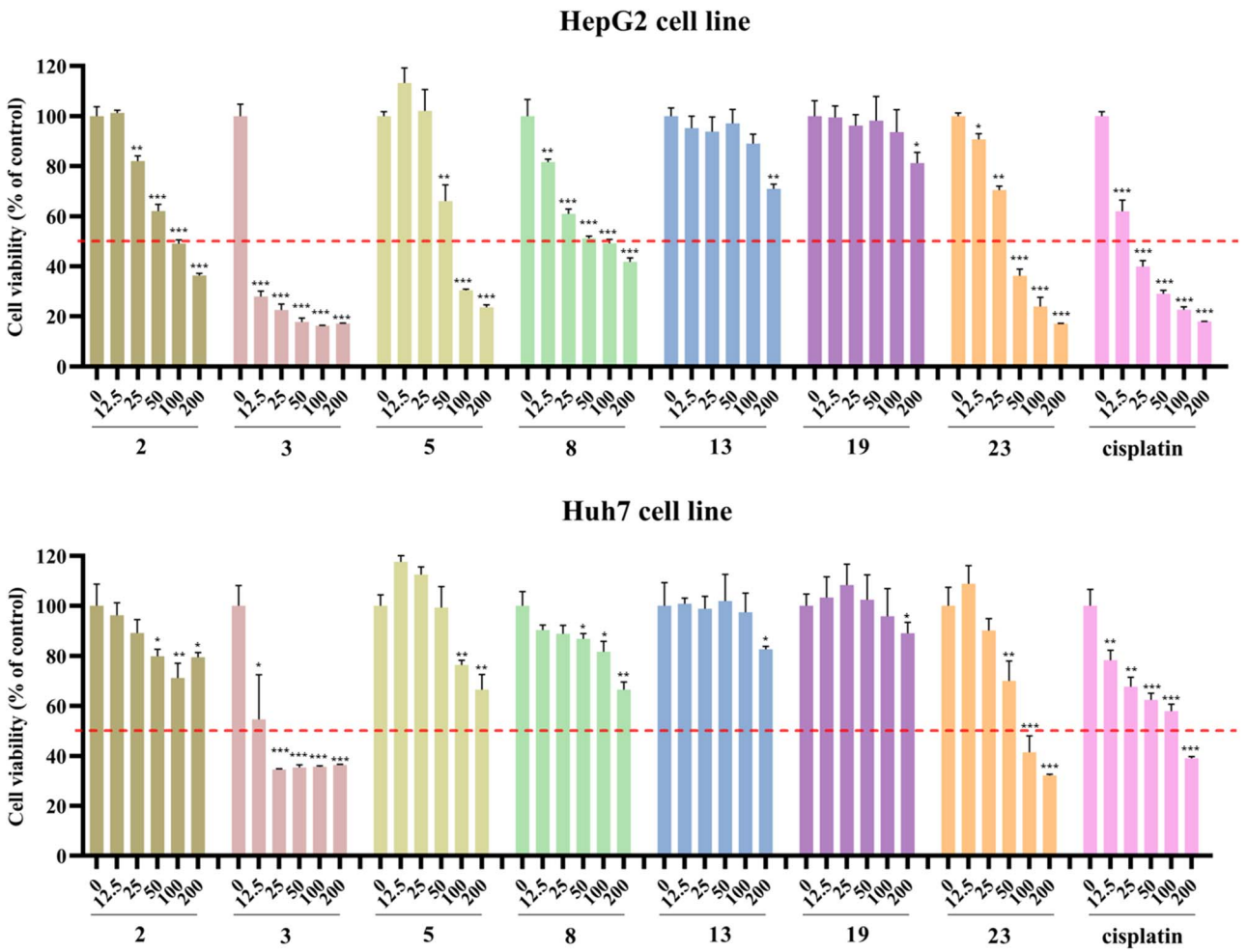

Fig. 5 Anti-hepatocarcinoma activities of compounds **2**, **3**, **5**, **8**, **13**, **19**, and **23**, with cisplatin as the positive control. Data were presented as mean ± SD of three parallel measurements. *p < 0.05, **p < 0.01, ***p < 0.001 *versus* the control group.

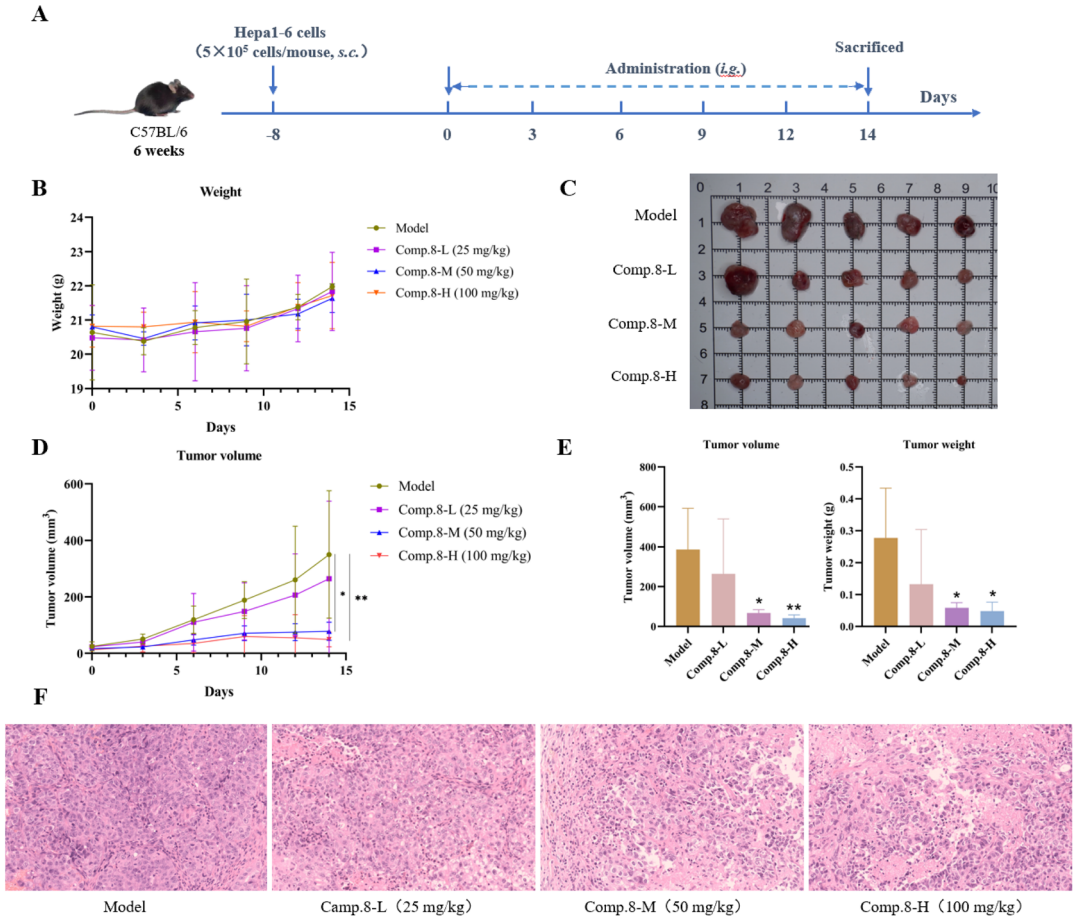

Fig. 6 Anti-hepatocarcinoma activity of Comp. **8** *in vivo*. (A) Schematic design of **8** *in vivo* anti-tumor effect study. (B) Changes in body weight of mice. (C) Images of the tumors from all mice at the endpoint. (D) Changes in the tumor volume of mice. (E) Tumor volume and weight changes after **8** treatment. (F) H&E staining of tumor tissue (scale bar = 100 μm). All data are shown as mean ± SD ($n = 5$). *$p < 0.05$, **$p < 0.01$, *versus* the model group.

2.3 Anti-hepatocarcinoma activity of compound 8 *in vivo*

Given its potent *in vitro* anti-hepatocarcinoma activity against HepG2 cells and sufficient yield from isolation, compound **8** was selected for further *in vivo* evaluation using a subcutaneous Hepa1-6 xenograft mouse model, as depicted in Fig. 6A. Compared to the model group, there was no significant change in the body weight of mice treated with **8** ($p > 0.05$), suggesting that the mice exhibited a favorable tolerance to **8** (Fig. 6B). The result was important as it demonstrated the safety profile of **8** with no apparent toxicity or adverse effects on overall health. As shown in Fig. 6C–E, tumor growth inhibition was observed in the medium and high dose groups, with significant reductions in both tumor volume and weight compared to the model group. At the doses of 25, 50, and 100 mg kg^{-1}, the tumor inhibition rates were 52.13%, 78.88%, and 82.70%, respectively, which demonstrated a dose-dependent anti-hepatocarcinoma effect of **8** *in vivo*. Histopathological examination using H&E staining (Fig. 6F) provided further insights into the cellular effects of **8** on tumor tissues. In the model group, the tumor cell structure remained intact with deeply stained nuclei. In contrast, tumor tissues from the medium and high dose groups showed vacuole-like degeneration, unclear cell membrane boundaries, and irregular nuclear enlargement, with the presence of necrosis and nuclear deformation.

Combined with the *in vitro* results, these findings provided evidence that **8** exerted significant anti-hepatocarcinoma effects. Further elucidation of the underlying molecular mechanisms and signaling pathways will contribute to a deeper understanding of its therapeutic mechanisms.

3 Experimental section

3.1 General experimental procedures

IR spectra were measured on a Bruker TENSOR37 infrared spectrometer with KBr disks. UV spectra were acquired on a Yokechina double-beam ultraviolet-visible spectrophotometer. Optical rotations were recorded on an Autopol l automatic polarimeter (Rudolph Research Analytical). 1D and 2D NMR spectra were obtained on a Bruker Ascend 600 NMR spectrometer with TMS as an internal reference. HR-ESI-MS were obtained on an Agilent 1290 Infinity LC and an Agilent 6530 Q-TOF mass spectrometer (Agilent, Palo Alto, CA, USA). Column chromatography (CC) was performed with silica gel (80–100

mesh, Huanghai, China). Medium-pressure liquid chromatography (MPLC) was performed using an RP-18 column (YMC C_{18}, 46 × 600 mm, 40–60 μm particle size) on a RUlHE LC-2100 liquid chromatography instrument. Semi-preparative HPLC purifications were conducted on a RUlHE LC-2010 liquid chromatography instrument with a Waters Xbridge Prep C_{18} column (10 × 250 mm, 5 μm) or an XSelect Prep C_{18} column (10 × 250 mm, 5 μm). Ultra Performance Liquid Chromatography (UPLC) was performed on the Waters XSelect Premier HSS T3 column (100 mm × 2.0 mm, 2.2 μm).

The HPLC-grade solvents (methanol and acetonitrile) were obtained from Thermo Fisher Scientific (Suwanee, GA, USA). Petroleum ether, ethyl acetate, methanol, and acetonitrile were acquired from Ghtech (Guangzhou, China). Deuterated chloroform ($CDCl_3$) was purchased from Macklin (Shanghai, China). The Cell Count Kit-8 (CCK-8) was purchased from Beyotime (Shanghai, China). Dulbecco's modified Eagle medium (DMEM), RPML-1640, 0.25% trypsin-ethylene diamine tetraacetic acid (EDTA) solution, penicillin–streptomycin solution, and phosphate buffer saline (PBS) were purchased from Servicebio (Wuhan, China). Fetal bovine serum (FBS) was obtained from Gibco (WalthamMA, USA).

3.2 Plant materials

The collection and identification of the aerial parts of *I. serra* were consistent with our previous study.[18]

3.3 Extraction and isolation

As recorded in our earlier study,[18] 80 kg of the aerial parts of *I. serra* were powdered and extracted with 80% EtOH (320 L) under reflux three times. The extracts were concentrated and then partitioned successively with petroleum ether (PE), ethyl acetate (EA), and aqueous solution (AS). The EA fraction (672 g) was subjected to silica gel CC using a gradient of PE–EtOAc–MeOH (1 : 0 : 0–0 : 0 : 1, v/v/v) to obtain eight fractions (Fr.A–H). Fr.C (62.7 g) was further separated by MPLC and eluted with a stepwise gradient of ACN–H_2O (10 : 90–100 : 0, v/v) to yield eight subfractions (Fr.C1–C8). Fr.C4 was purified by semi-preparative HPLC eluted with MeOH–H_2O (40 : 60) to yield compounds **1** (10.40 mg) and **4** (51.82 mg). Similarly, compound **5** (60.23 mg) was purified from Fr.C5 using semi-preparative HPLC (MeOH–H_2O, 49 : 51). Fr.C6 was separated *via* semi-preparative HPLC eluted with MeOH–H_2O (58 : 42) to afford compounds **6** (30.09 mg) and **7** (30.76 mg). Compound **8** (2.24 g) was obtained from Fr.C7 by repeated recrystallization using MeOH. Fr.E (53.0 g) was chromatographed on a C_{18} MPLC column eluted with a gradient of ACN–H_2O (15 : 85–100 : 0, v/v) to give ten subfractions, Fr.E1-E10. Compound **16** (20.36 mg) was acquired using recrystallization from Fr.E2. The residue of Fr.E2 was purified using semi-preparative HPLC eluted with MeOH–H_2O (41 : 59) to afford compounds **17** (7.38 mg). Following, Fr.E3 was isolated by MPLC and eluted with MeOH–H_2O (35 : 65–54 : 46, v/v) to obtain two subfractions (Fr.E3-a and E3-b). Fr.E3-a and Fr.E3-b were respectively subjected to semi-preparative HPLC (MeOH–H_2O, 43 : 57 and 50 : 50) to obtain compounds **21** (10.27 mg) and **3** (35.81 mg). Compound **9** (107.24 mg) was obtained from Fr.E4 by repeated recrystallization using MeOH. The residue of Fr.E4 was subjected to sim-PHPLC (MeOH–H_2O, 48 : 52) to yield compound **10** (8.26 mg). Fr.E5 was purified by semi-preparative HPLC (MeOH–H_2O, 54 : 46) to give compounds **18** (10.32 mg) and **19** (28.65 mg). Compound **11** (98.04 mg) was afforded from Fr.E6 by sim-PHPLC (MeOH–H_2O, 58 : 42). Fr.E7 (1.88 g) was further separated by MPLC and eluted with a stepwise gradient of 54–78% MeOH in H_2O to provide seven subfractions, Fr.E7-a–E7-g. Fr.E7-b was further purified by HPLC eluted with MeOH–H_2O (58 : 42) to yield compound **22** (18.23 mg). Fr.E7-c was separated *via* semi-preparative HPLC (MeOH–H_2O, 61 : 39) to afford compound **23** (19.26 mg). Similarly, compounds **12** (15.17 mg) and **20** (25.02 mg) were isolated from Fr.E7-d by semi-preparative HPLC (MeOH–H_2O, 65 : 35). Compound **13** (162.37 mg) was isolated from Fr.E7-f by repeated recrystallization using MeOH. Fr.E7-g was further purified by HPLC eluted with MeOH–H_2O (72 : 28) to provide compound **14** (55.66 mg). Fr.E9 was separated by an MPLC column and eluted with MeOH–H_2O (70 : 30–80 : 20, v/v) to afford four fractions (Fr.E9-a–E9-d). Fr.E9-c was separated *via* semi-preparative HPLC (MeOH–H_2O, 72 : 28) to afford compound **15** (21.61 mg). Fr.E0-d was purified by semi-preparative HPLC (MeOH–H_2O, 75 : 25) to give compound **2** (48.2 mg).

Isodosin E (**1**): light yellow powder; $[\alpha]_D^{21.4}$ −360.72 (c = 0.5, MeOH); UV (MeOH) λ_{max} (log ε) 210 (3.54), 295 (2.64), 320 (2.64) nm; IR (KBr) ν_{max} 3479, 2935, 1738, 1371, 1248, 1021 cm^{-1}; ^1H and ^{13}C NMR, see Table 1; HR-ESI-MS m/z 413.1950 $[M + Na]^+$ (calcd for $C_{22}H_{30}O_6Na$, 413.1935).

Isodosin F (**2**): white amorphous powder; $[\alpha]_D^{21.8}$ −29.88 (c = 0.5, CH_2Cl_2); UV (MeOH) λ_{max} (log ε) 210 (3.64), 281 (3.00) nm; IR (KBr) ν_{max} 3263, 2924, 1718, 1241, 1162 cm^{-1}; ^1H and ^{13}C NMR, see Table 1; HR-ESI-MS m/z 437.2569 $[M + H]^+$ (calcd for $C_{24}H_{36}O_7H$, 437.2534).

Isodosin G (**3**): white amorphous powder; $[\alpha]_D^{21.8}$ −86.96 (c = 0.5, MeOH); UV (MeOH) λ_{max} (log ε) 211 (3.54) nm; IR (KBr) ν_{max} 2906, 1696, 1232, 1121, 1042 cm^{-1}; ^1H and ^{13}C NMR, see Table 1; HR-ESI-MS m/z 385.1630 $[M + Na]^+$ (calcd for $C_{20}H_{26}O_6Na$, 385.1622).

3.4 ECD calculations

ECD calculations were carried out as previously reported, with appropriate modifications.[18] The conformational analyses were performed using random searches in Spartan 16 (Wavenfunction, lrvine, CA, USA, 2016) with the MMFF94 force field. The conformers were then re-optimized using DFT at the B3LYP/6-31G(d,p) level using Gaussian 09 with the SMD model. For all conformers with Boltzmann populations exceeding 1%, energies, oscillator strengths, and rotational strengths (velocity) were subsequently computed *via* TDDFT at the B3LYP/6-311+g(d,p) level in MeOH. The ECD spectra were simulated by Gaussian convolution (σ = 0.30) before being averaged according to their Boltzmann distribution theory and relative Gibbs free energy (ΔG) values.

3.5 Cell lines and cell culture

Human hepatocellular carcinoma HepG2 and Huh7 cell lines, as well as the murine hepatoma Hepa1-6 cell line, were obtained from the American Type Culture Collection (ATCC, Manassas,

VA, USA). They were cultured in DMEM medium supplemented with 10% FBS and 1% antibiotics (penicillin and streptomycin) at 37 °C in a humidified 5% CO_2 incubator.

3.6 Anti-hepatocarcinoma assay *in vitro*

The anti-hepatocarcinoma activities of the main compounds **2**, **3**, **5**, **8**, **13**, **19**, and **23**, along with the positive control cisplatin, were evaluated using the CCK-8 assay. Briefly, HepG2 and Huh7 cells were seeded in 96-well plates at a density of 5×10^3 cells per well and incubated for 24 h. The cells were then treated with various concentrations (0, 12.5, 25, 50, 100, and 200 μM) of selected compounds and cisplatin. After a further 24 h incubation, 10 μL of CCK-8 solution was added and the cells were incubated at 37 °C for 4 h. Finally, the absorbance at 450 nm was measured using a Multiskan SkyHigh Spectrum (Thermo Scientific™, Waltham, MA, USA).

3.7 Animals and experimental protocols

All animal procedures were performed in accordance with the Guidelines for Care and Use of Laboratory Animals of Guangdong Pharmaceutical University and approved by the Animal Ethics Committee of Guangdong Pharmaceutical University (No. gdpulacspf2022559). Six-week-old male C57BL/6 mice were purchased from the Experimental Animals Center of Guangdong Province, China. Animals were housed at a temperature of 23–25 °C and relative humidity of (50 ± 10)% with a 12 hours of light and dark cycle. After a week of acclimation, the mice were subcutaneously injected with 5×10^5 Hepa1-6 cells (0.1 mL per mouse) in the right axillary. The mice were randomly divided into four groups ($n = 5$): model, Comp. **8**-L group (*i.g.*, 25 mg kg^{-1}), Comp. **8**-M group (*i.g.*, 50 mg kg^{-1}), and Comp. **8**-H group (*i.g.*, 100 mg kg^{-1}). Mice in Comp. **8** treated groups were administered different doses of Comp. **8** (dissolved in 0.5% CMC-Na) by *i.g.* administration once daily for 14 days, and the model mice received the same volume of 0.5% CMC-Na. The size of the tumors was measured every 3 days with calipers, and the tumor volume was calculated using the formula, volume (mm^3) = (length × $width^2$)/2. At the end of the administration, mice were anesthetized and euthanized by cervical dislocation, and tumors were immediately removed, measured, and weighed.

3.8 H&E staining

To evaluate histological alterations, tumor tissues were fixed with 4% paraformaldehyde, embedded in paraffin, and cut into 5 μm sections. Sections were then stained with hematoxylin and eosin (H&E). Finally, the stained sections were examined under a light microscope.

3.9 Statistical analysis

All data were expressed as mean ± standard deviation (mean ± SD). Statistical analysis was performed using GraphPad Prism, Version 8.2.1 (GraphPad Software, Inc., San Diego, CA, USA) with a one-way analysis of variance (ANOVA) test. A value of $p < 0.05$ was considered statistically significant.

4 Conclusions

In summary, three new diterpenoids, including two 7,20-epoxy-*ent*-kaurane type diterpenoids (**1–2**) and one enmein-type *ent*-kaurane diterpenoid (**3**), together with 20 known diterpenoids (**4–23**), were isolated from the aerial parts of *I. serra.* The anti-hepatocarcinoma activities of the main compounds were evaluated against HepG2 and Huh7 cells, with compounds **3**, **8**, and **23** demonstrating significant inhibition effects on HepG2 cells. Moreover, compound **8** exhibited significant inhibition of tumor growth *in vivo*. These findings not only enriched the chemical composition of *I. serra*, but also supported the potential application of these diterpenoids in the therapy of HCC.

Data availability

The raw data supporting the conclusions will be made available by the authors upon request.

Author contributions

J. Yang conceived and designed the experiments; H. L. Wu contributed to the isolation, structure elucidation, and writing. C. Liu, S. Q. Li, and S. X. Wang contributed to the biological activity test; Z. Y. Huang and Y. H. Xu prepared the ESI;† X. He, C. C Zhang, and J. Ma revised the manuscript; X. He and G. Yang contributed to project management and funding acquisitions. All authors have read and agreed to the published version of the manuscript.

Conflicts of interest

The authors declare no conflicts of interest.

Acknowledgements

This research was funded by the Scientific Research Projects of Guangdong Provincial Bureau of Traditional Chinese Medicine (Grant No. 20241168, 20231206), the Science and Technology Planning Project of Guangzhou (Grant No. SL2022A04J00771, SL2023A04J02377), the Medical Scientific Research Foundation of Guangdong Province (Grant No. A2024479), the Guangdong Basic and Applied Basic Research Foundation (Grant No. 2022A1515110678), the National Natural Science Foundation of China (Grant No. 82304859), the Key Research and Development Program of Shanxi (Grant No. 2021ZDLSF04-03), and the CACMS Innovation Fund (Grant No. CI2021A03907).

Notes and references

1 M. Liu, W. G. Wang, H. D. Sun and J. X. Pu, *Nat. Prod. Rep.*, 2017, **34**, 1090–1140.
2 H. D. Sun, S. X. Huang and Q. B. Han, *Nat. Prod. Rep.*, 2006, **23**, 673–698.

3 C. L. Qiu, Z. N. Ye, B. C. Yan, K. Hu, J. Yang, X. Z. Yang, H. M. Li, X. N. Li, H. D. Sun and P. T. Puno, *Bioorg. Chem.*, 2022, **124**, 105811.
4 Y. X. Li, J. Chi, L. X. Zhang, F. Wang, W. J. Zhang, Z. M. Wang and L. P. Dai, *Phytochemistry*, 2024, **228**, 114247.
5 M. A. Ali, N. Khan, A. Ali, H. Akram, N. Zafar, K. Imran, T. Khan, K. Khan, M. Armaghan, M. Palma-Morales, C. Rodríguez-Pérez, A. Caunii, M. Butnariu, S. Habtemariam and J. Sharifi-Rad, *Food Sci. Nutr.*, 2024, **12**, 3046–3067.
6 X. Zhong, H. Liao, S. Hu, K. Luo and H. Zhu, *Mol. Cell. Probes*, 2021, **59**, 101759.
7 L. Gou, G. G. Yue, J. K. Lee, P. T. Puno and C. B. Lau, *Biochem. Pharmacol.*, 2023, **210**, 115491.
8 P. J. M. Sobral, A. T. S. Vicente and J. A. R. Salvador, *Front. Chem.*, 2023, **11**, 1066280.
9 H. Wang, Y. Ye and Z. L. Yu, *Oncol. Rep.*, 2014, **31**, 2165–2172.
10 X. Hu, S. Huang, S. Ye and J. Jiang, *Curr. Pharm. Biotechnol.*, 2024, **25**, 655–664.
11 Y. Ding, C. Ding, N. Ye, Z. Liu, E. A. Wold, H. Chen, C. Wild, Q. Shen and J. Zhou, *Eur. J. Med. Chem.*, 2016, **122**, 102–117.
12 J. Wan, M. Liu, H. Y. Jiang, J. Yang, X. Du, X. N. Li, W. G. Wang, Y. Li, J. X. Pu and H. D. Sun, *Phytochemistry*, 2016, **130**, 244–251.
13 H. Xing, L. An, Z. Song, S. Li, H. Wang, C. Wang, J. Zhang, M. Tuerhong, M. Abudukeremu, D. Li, D. Lee, J. Xu, N. Lall and Y. Guo, *J. Nat. Prod.*, 2020, **83**, 2844–2853.
14 R. J. Xie, F. L. Yan, G. F. Hai, R. J. Hou, M. M. Ding and Y. X. Bai, *Fitoterapia*, 2011, **82**, 726–730.
15 Q. Zheng, J. Cui and H. Fu, *Zhongguo Zhongyao Zazhi*, 2011, **36**, 2203–2206.
16 X. Liu, Z. Bian, Y. Tian, H. Li, S. Hu, C. Li, P. Pandey, D. Ferreira, A. G. Chittiboyina, M. T. Hamann, X. Ma, S. Wang and X. Wang, *Fitoterapia*, 2024, **176**, 106019.
17 J. J. Hu, B. L. Li, J. D. Xie, H. J. Liang, Q. R. Li, J. Yuan and J. W. Wu, *Nat. Prod. Res.*, 2022, **36**, 2021–2027.
18 S. Li, F. Liang, D. Huang, H. Wu, X. Tan, J. Ma, C. Wei, S. Wang, Z. Huang, G. Yang, X. He and J. Yang, *Molecules*, 2024, **29**, 2733.
19 E. Fujita, T. Fujita, M. Shibuya and T. Shingu, *Tetrahedron*, 1969, **25**, 2517–2530.
20 Z. R. Ping, Z. Hongjie, L. Zhongwen, Z. Yulin and S. Handong, *Phytochemistry*, 1992, **31**, 4237–4240.
21 X. M. Niu, S. H. Li, M. L. Li, Q. S. Zhao, S. X. Mei, Z. Na, S. J. Wang, Z. W. Lin and H. D. Sun, *Planta Med.*, 2002, **68**, 528–533.
22 C. Tao, Q. J. Li, L. H. Ye, J. X. Zhang and X. S. Yang, *Nat. Prod. Res. Dev.*, 2015, **27**, 26–30.
23 L. M. Li, G. Y. Li, S. X. Huang, S. H. Li, Y. Zhou, W. L. Xiao, L. G. Lou, L. S. Ding and H. D. Sun, *J. Nat. Prod.*, 2006, **69**, 645–649.
24 B. L. Li, J. Li, L. Tong, Y. J. Pan and K. B. Yu, *Bull. Korean Chem. Soc.*, 2004, **25**, 304–306.
25 T. Fujita, Y. Takeda, T. Shingu and A. Ueno, *Chem. Lett.*, 1980, **9**, 1635–1638.
26 W.-G. Wang, J. Yang, H.-y. Wu, L.-M. Kong, J. Su, X.-N. Li, D. Xue, R. Zhan, Z. Min, Y. Li, J. Pu and H.-D. Sun, *Tetrahedron*, 2015, **71**, 9161–9171.
27 Y. Takeda, T. Fujita, H.-d. Sun, Y. Minami, M. Ochi and C.-C. Chen, *Chem. Pharm. Bull.*, 1990, **38**, 1877–1880.
28 B. Li, Y.-J. J. Pan and W. Pan, *Helv. Chim. Acta*, 2001, **84**, 3418–3422.
29 Z. M. Wang, H. Feng, X. T. Liang, S. T. Yuan and M. J. Xu, *Acta Pharm. Sin.*, 1996, 764–769.
30 L. Gou, K. Hu, Q.-F. Yang, X.-N. Li, H.-D. Sun, C. L. Xiang and P. T. Puno, *Tetrahedron*, 2019, **75**, 2797–2806.
31 Y. H. Shen, Z. Y. Wen, G. Xu, W. L. Xiao, L. Y. Peng, Z. W. Lin and H. D. Sun, *Chem. Biodiversity*, 2005, **2**, 1665–1672.
32 K. Kakinuma, Y. Okada, N. Ikekawa, T. Kada and M. Nomoto, *Agric. Biol. Chem.*, 1984, **48**, 1647–1648.
33 F. L. Yan, L. Guo, S. Bai and H.-D. Sun, *J. Chin. Chem. Soc.*, 2008, **55**, 933–936.
34 F. L. Yan, L. Q. Guo, J. X. Zhang, S. P. Bai and H. D. Sun, *Chin. Chem. Lett.*, 2008, **19**, 441–443.
35 S. N. Chen, Z. W. Lin, G. W. Qin, H. D. Sun and Y. Z. Chen, *Planta Med.*, 1999, **65**, 472–474.
36 Y. X. Wu, F. Ye, W. Zhang, J. C. Li and N. Liu, *China J. Chin. Mater. Med.*, 2011, **36**, 1772–1775.
37 Q. B. Han, M. L. Li, S. H. Li, Y. K. Mou, Z. W. Lin and H. D. Sun, *Chem. Pharm. Bull.*, 2003, **51**, 790–793.
38 X. M. Gao, X. Luo, J. X. Pu, Y. L. Wu, Y. Zhao, L. B. Yang, F. He, X. N. Li, W. L. Xiao, G. Q. Chen and H. D. Sun, *Planta Med.*, 2011, **77**, 169–174.
39 F. Bray, M. Laversanne, H. Sung, J. Ferlay, R. L. Siegel, I. Soerjomataram and A. Jemal, *Ca-Cancer J. Clin.*, 2024, **74**, 229–263.
40 S. Chidambaranathan-Reghupaty, P. B. Fisher and D. Sarkar, *Adv. Cancer Res.*, 2021, **149**, 1–61.
41 W. Tang, Z. Chen, W. Zhang, Y. Cheng, B. Zhang, F. Wu, Q. Wang, S. Wang, D. Rong, F. P. Reiter, E. N. De Toni and X. Wang, *Signal Transduction Targeted Ther.*, 2020, **5**, 87.
42 D. Anwanwan, S. K. Singh, S. Singh, V. Saikam and R. Singh, *Biochim. Biophys. Acta, Rev. Cancer*, 2020, **1873**, 188314.